Electrode permeability and flow-field configuration: influence on the performance of a PEMFC

J. Soler[a], E. Hontañón[a], L. Daza[a,b,*]

[a]*Dpto. Combustibles Fósiles, CIEMAT, Av. Complutense 22, 28040 Madrid, Spain*
[b]*Instituto de Catálisis y Petroleoquímica, CSIC, Cantoblanco, 28049 Madrid, Spain*

Abstract

The objective of this work was to investigate the effect of both the permeability of the electrodes and the configuration of the gas flow distributor on the performance of a proton exchange membrane fuel cell (PEMFC). For that purpose, MEAs including electrodes of two types, carbon paper and carbon cloth, have been characterised electrochemically by measuring the polarization curves for a wide range of operational conditions with H_2 and O_2/air as reactants. MEAs with surface active areas of 50 and 290 cm^2 have been characterised in single cells with two flow-field configurations: a grooved plate with parallel gas channels and solid ribs, and a solid plate. The latter is a novel gas flow distributor that has been designed and tested in our laboratory. A subsequent series of experiments were carried out in order to measure the gas permeability of the electrodes of the MEAs characterised previously. The permeability of the electrodes was measured separately for O_2, N_2 and H_2 in the absence of water vapour.

The fuel cell performance strongly depends on both the gas permeability of the electrodes and the type of gas flow distributor. The effect of the electrode permeability is not meaningful in the case of the grooved plates, but it is rather important in the case of the solid plates. With the grooved plates, the differences in the fuel cell performance observed with the various MEAs must be attributed to factors mostly related to the catalyst layer (platinum and Nafion content, dispersion of the catalyst, etc.). With solid plates, however, the MEAs of both short and large sizes performed consistently with the gas permeability values of the electrodes measured in this work. In general, the performance of the fuel cell with solid plates declines when the permeability of the electrodes decreases. In the range of current densities covered here, below 300 mA/cm^2, the MEAs with the more permeable electrodes performed comparably with either grooved or solid plates. The less permeable electrodes were the ones in the MEAs provided by E-TEK, which are made of carbon cloth with 40 wt.% of hydrophobic material. In this case, noticeably higher gas transport losses were observed with the solid plates than with the grooved plates, particularly when air was used as oxidant.

The influence of water vapour on the gas electrode permeability and the effect of the electrode hydraulic permeability on the fuel cell performance will be investigated in a future work.
© 2003 Elsevier Science B.V. All rights reserved.

Keywords: PEMFC; Proton exchange membrane fuel cells; Electrode permeability; Flow-field configuration; Bipolar plates

1. Introduction

In the proton exchange membrane fuel cells (PEMFC) the electrodes are made of a porous mixture of carbon supported platinum and ionomer. In order to be able to catalyse reactions, catalysts particles must have contact to both protonic and electronic conductors. Furthermore, there must be passages for reactants to reach the catalyst sites and for reaction products to exit. The contacting point of the reactants, catalyst and electrolyte is conventionally referred to as the three-phase interface. The porous backing layer, which is placed behind the catalyst layer, fulfils important tasks in the PEMFC. In this layer, combined requirements of effective reactant gas supply

to the catalyst layer and effective water supply and removal in either vapour or liquid form have to be simultaneously fulfilled. Wet-proofing by PTFE is required to ensure that at least part of the pore volume in the cathode backing remains free of liquid water in an operating cell, so as to enable rapid gas-phase transport. The scale of the porosity and the amount of PTFE added are two important parameters that determine the success of the backing layer in fulfilling the combined tasks of gas and water transport. Obviously, the backing layer has to be made of a material of high and stable electronic conductivity in a wet environment. Although some expanded metal structures have been suggested, most of PEMFC backings to date have been based on porous carbon paper [1–5], or cloth [6–9]. The effect of the electrode backing material on the fuel cell performance has been investigated in previous works [10–12]. In general, MEAs with carbon cloth electrodes has

better performance that the ones with paper diffuser at higher current densities, whereas MEAs with paper diffuser are better at lower current densities. Some authors [12] attribute that behaviour to lower Ohmic losses for paper at lower current densities compared to cloth, while cloth has lower diffusion losses at high current densities. The aim of this work was to investigate the influence of the backing gas permeability and the flow-field pattern on the performance of a PEMFC. These two factors determine the distribution of the reactants on the surface of the electrodes as well as the total

flow rate of gases that reaches the catalytic layer, with the subsequent impact on the fuel cell performance.

2. Experimental

The experimental activities accomplished in this work are described in this section. Firstly, a series of MEAs of different sizes and electrodes, as summarised in Table 1, were characterised electrochemically. The polarisation
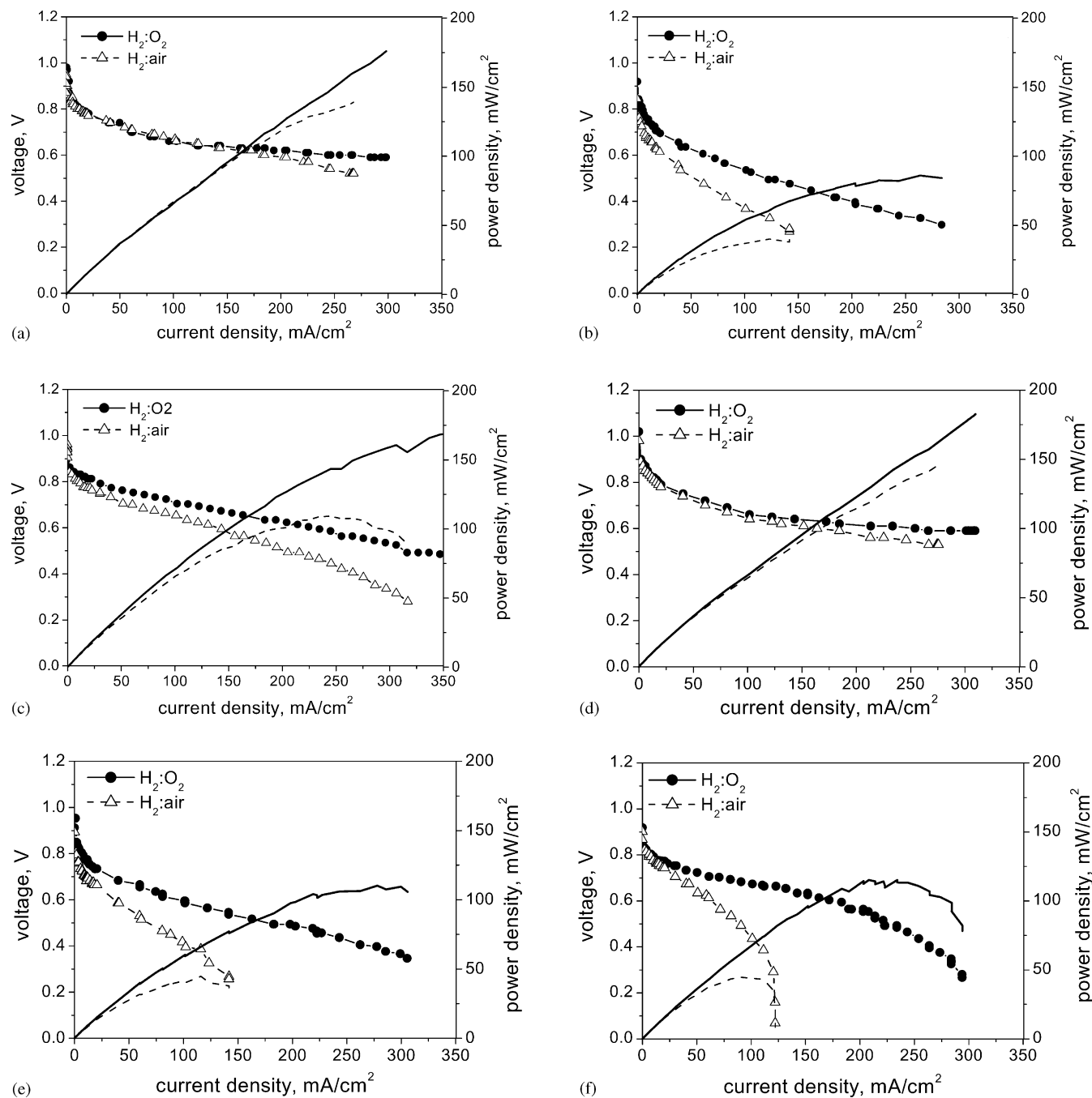

Fig. 1. Polarisation curves obtained with MEAs of 50 cm^2 active area and two gas flow distributors. Grooved plate: (a) EC, (b) SH2, (c) E-TEK1. Solid plate: (d) EC, (e) SH2, (f) E-TEK1. The material of the electrode was carbon paper (a, d), and carbon cloth (b, e, c, f).

curves of the MEAs were obtained in single cells for a wide range of operational conditions. Then, the gas permeability of the electrodes of the MEAs characterised previously was measured experimentally.

2.1. Polarisation curves

The measurement of the performance of the MEAs was carried out in an experimental device that consists of a set of mass flow controllers to feed the reactant gases to both the anodic and cathodic sides. The mixtures of gases pass through humidifiers, which are filled by means of a peristaltic pump. The gases continue along a heater pipe and are injected in the fuel cell, which is heated by an external electrical power source with a PID controller. The water from the exhausted gases is condensed before being removed and the dry gases pass through pressure valves which let fix overpressure in the fuel cell. The control and the data acquisition are made by means of specific PC software developed in our laboratory. For the load demand, a resistive load (HP 6060B) with a range of 3–60 V and 0–60 A was used originally. Due to the internal resistance of the load (30 Ω), in the experiments with single cells a maximum current intensity of 15 A was achieved at fuel cell voltages nearly 0.5 V. Later on, the electronic load was substituted by a bipolar power supply (Fug NLB700M-6.5) in the range from 0 to $\pm$60 A and 0 to $\pm$6.5 V, which allowed to overcome the previous limitations.

MEAs of two sizes, 50 and 290 cm^2, were tested in single cells with two different gas flow distributors: a ribbed plate and a solid plate. These configurations were mechanized on two graphite plates which were assembled in a monocell arrangement. A simple calculation, based on first principles, was performed in order to determine the force couple necessary to obtain a good electric contact: 3.4 N m in the case of the short MEAs (50 cm^2) and 10.2 N m for the large ones (290 cm^2).

A wide range of gas flow rates and pressures was covered in the characterisation experiments, with H$_2$ as fuel and either O$_2$ or air as oxidant. In order to compare, the gas flow rates for testing the MEAs were as following for electrodes: (a) 50 cm^2: H$_2$ (0.4 l/min), O$_2$ (0.4 l/min) for tests H$_2$:O$_2$ and H$_2$ (0.4 l/min), O$_2$ (0.4 l/min), N$_2$ (1.5 l/min) for tests H$_2$:air; (b) 290 cm^2: H$_2$ (0.8 l/min), O$_2$ (0.4 l/min) for test H$_2$:O$_2$ and H$_2$ (0.8 l/min), O$_2$ (0.4 l/min), N$_2$ (1.5 l/min) for tests H$_2$:air. The fuel cell temperature was maintained constant at 60 $^\circ$C in all the tests, and the gas humidification temperatures were 70 and 65 $^\circ$C in the anode and cathode, respectively. The internal resistance of the electronic load limited the maximum current density attainable in experiments with single cells, which explains the interruption of the polarization curves displayed in Figs. 1 and 2.

2.2. Electrode permeability

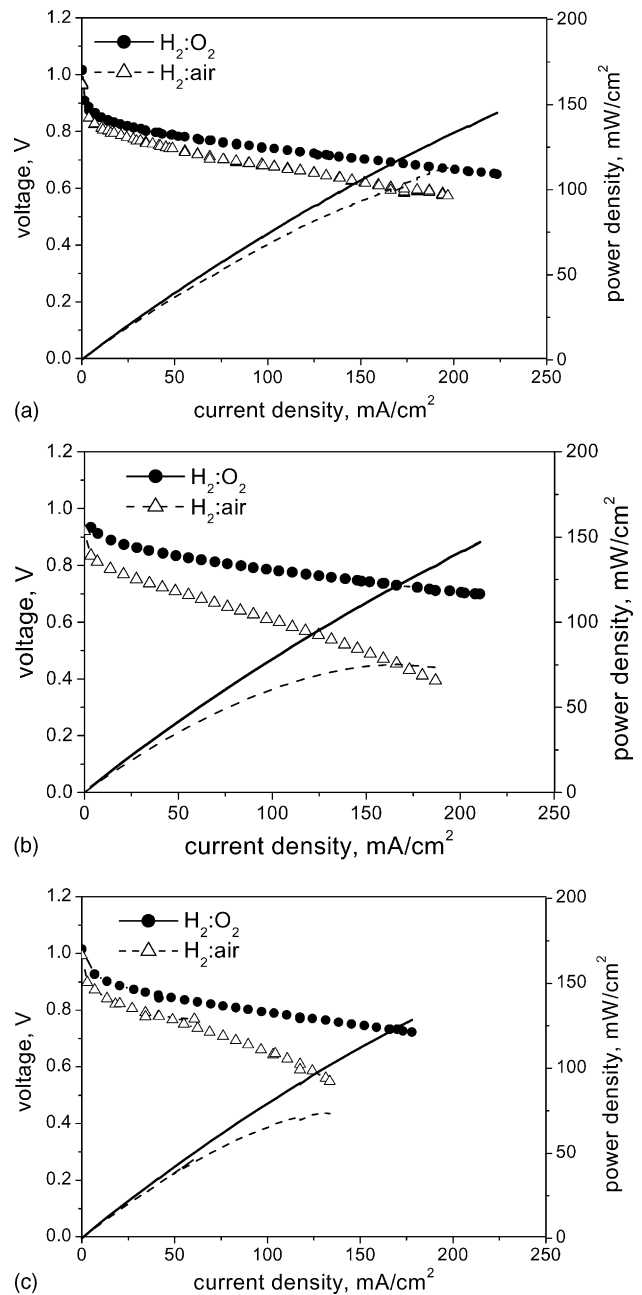The effective gas permeability of the electrodes of the MEAs was obtained by measuring the pressure drop as a

Fig. 2. Polarisation curves obtained with MEAs of 290 cm^2 active area. E-TEK2 and two flow-field configurations: (a) grooved plate, (b) solid plate, and (c) LA and solid plate as gas flow distributor.

function of the gas flow rate. The MEAs were assembled in a monocell configuration and were clamped at the same force couple that was used in the polarisation curve tests. Then, nitrogen, oxygen and hydrogen were fed sequentially into the anode and cathode sides of the MEAs. The reason to use these gases was to simulate the operational conditions that take place in a fuel cell. We measured the pressure drop along the electrodes for flow rates up to 2 l/min by means of a differential pressure transmitter (Spriano model SET 27B) with a nominal range between 0 and 250 mbar. The flow rate was incremented from 50 to 300 and 100 ml/min in the rest.

Table 1
Characteristics of the electrodes of the MEAs used in this work

MEAs	Electrode material	Hydrophobic ontent (wt.%)	Catalyst (wt.% Pt/C)	Platinum load (mgPt/cm^2)	Electrode thickness (mm)
50 cm^2					
EC	Carbon paper	–	20	1.0	0.25
SH1	Carbon paper	–	40	0.7	0.25
SH2	Carbon cloth	20	20	0.5	0.35
E-TEK1	Carbon cloth	40	20	0.5	0.35
290 cm^2					
LA	Carbon paper	–	40	0.7	0.25
E-TEK2	Carbon cloth	40	20	0.5	0.35

The electrolyte was a membrane of Nafion 117 in all the cases.

3. Results and discussion

In a previous work [13,14], using a 3D numerical simulation, the performance of the flow distributor was assessed in terms of the fuel consumption of the anode. Gas consumption increased when decreased the permeability of the gas distributor placed on the front of the electrode. The simulation showed that in terms of reactant utilisation, porous materials were more advantageous than grooved plates. Tests for both polarization curves and electrode permeability were made to confirm these results.

3.1. Polarization curves

Table 1 shows the characteristics of the MEAs used in this work; in all the cases the electrolyte was a membrane of Nafion 117. Commercial MEAs were purchased from ElectroChem (EC) and E-TEK. The rest of the MEAs were prepared using commercial components: short size (SH1 and SH2) and large size (LA). The polarisation curves displayed in Fig. 1 (electrode 50 cm^2) and Fig. 2 (electrode 290 cm^2) were measured in the conditions explained in Section 2.1. The internal resistance of the electronic load limited the maximum current density attainable in experiments with single cell (see Section 2.1), which explains the interruption of the polarization curves displayed in Figs. 1 and 2.

In the case of the MEAs with electrodes of 50 cm^2, with grooved plates, the best performance corresponds to the MEA EC followed of E-TEK1 and SH2. With solid plates, again the MEA EC performed the best followed of SH2 and E-TEK1. Moreover, the MEAs EC and SH2 showed similar performance with the two gas flow distributors, while the MEA E-TEK1 performed significantly better with grooved plates than with solid plates.

In the case of the MEAs with electrodes of 290 cm^2, for a given gas flow distributor, the MEAs LA and E-TEK2 performed comparably. No effect of the gas flow distributor on the fuel cell performance was observed with O$_2$. With air, however, better results were obtained with the grooved plate than with the solid one.

3.2. Electrode permeability

Measurements of the electrode gas permeability were undertaken in order to explain the electrochemical behaviour of the MEAs characterised in Section 3.1. The pressure drop was measured as a function of the gas flow rate in the two electrodes of the MEAs (e1 and e2) for N$_2$, O$_2$ and H$_2$ separately. The graphs obtained are plotted in Fig. 3. The pressure drop at a certain flow rate depends on the physical properties of the gas, mainly viscosity, which explains the different slope of the experimental data obtained with the three gases. The largest pressure drop corresponds to oxygen, closely followed of nitrogen. Lower pressure drop was measured with hydrogen, the lightest one. In general, the two electrodes of every MEA behaved comparably except for MEAs SH1 (Fig. 3a) and E-TEK1 (Fig. 3c). These discrepancies may be attributed to differences in the structure of the two electrodes: pore size distribution and connectivity, electrode thickness, etc., that could have emerged during the preparation of the MEAs. The experimental data were fitted to a straight line from which slope, the permeability of the electrodes was derived. The Darcy law relates the pressure drop and the velocity of a fluid in a porous medium. In the tests, the gas flows along the electrodes from the inlet to the outlet of the fuel cell, in both the anode and the cathode sides. Therefore, for the quadrangular MEAs used in this work, the Darcy's law takes the form

$$\bar{\nabla}P = \frac{\mu}{\alpha}\bar{V} \tag{1}$$

$$\Delta P = \frac{\mu}{K}\frac{Q}{L \cdot e}H \tag{2}$$

where ΔP represents the pressure drop along the electrode; H, L and e are, respectively, the length, height and thickness of the electrode; Q is gas flow rate; K represents the lateral permeability of the electrode; and μ is the gas molecular viscosity.

Due to the fact that MEAs were prepared using the hot pressing technique and to the compression they withstood inside the fuel cell during the characterisation phase, the real thickness of the electrodes was not known. Thus, instead of
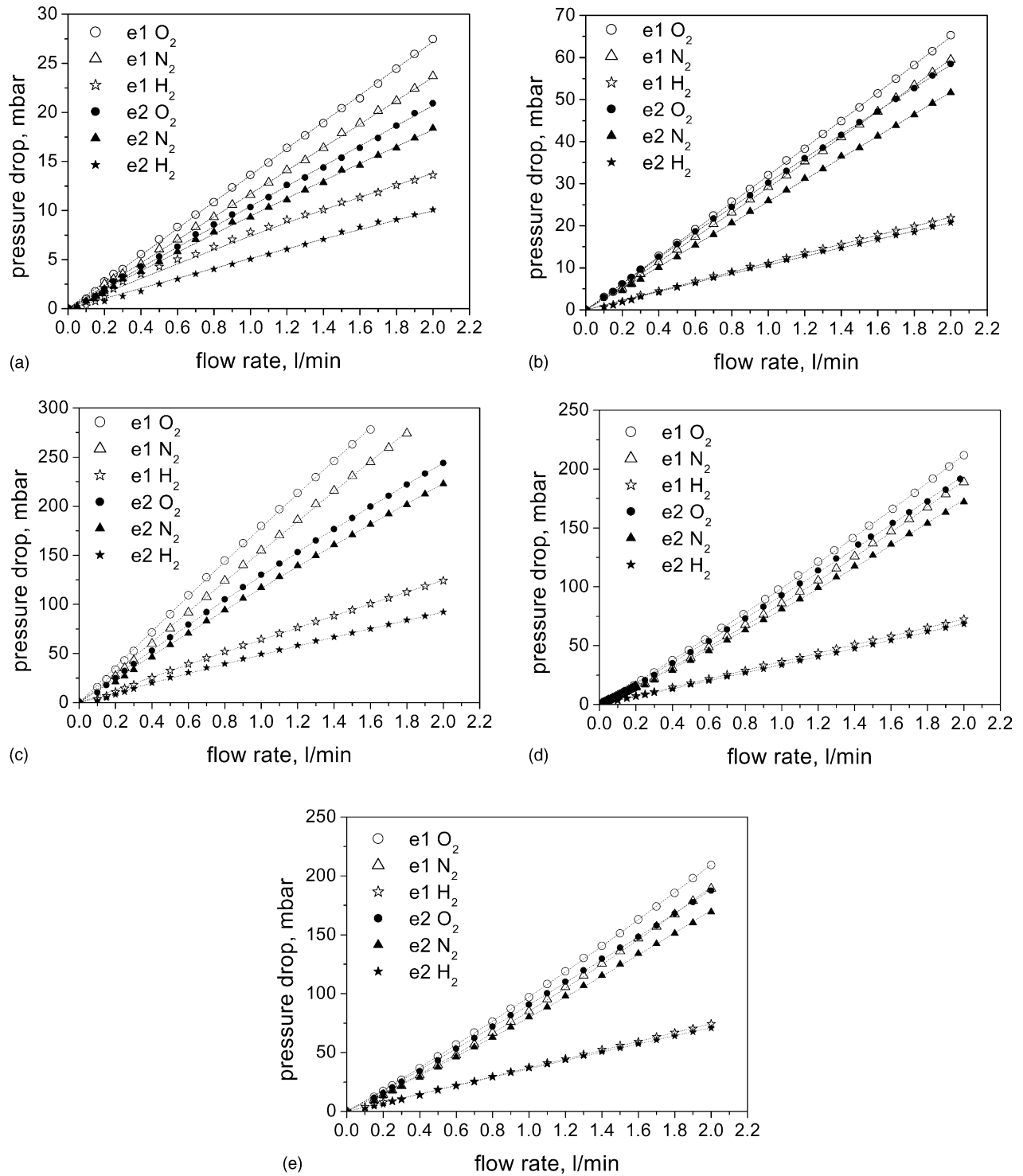
Fig. 3. Pressure drop vs. gas flow rate in the electrodes of the MEAs. Active areas: 50 cm^2: (a) SH1, (b) SH2, (c) E-TEK1; 290 cm^2: (d) LA, (e) E-TEK2.

K we calculated the product $K \cdot e$ that, in any case, serves to compare the permeability of the electrodes of the different MEAs. The product $K \cdot e$ was estimated with the expression

$$K \cdot e = \frac{\mu}{S} \frac{H}{L} \frac{1}{101325 \times 6 \times 10^4} \frac{T}{273} \qquad (3)$$

with S the slope of the lines and T the room temperature.

The $K \cdot e$ values so obtained are shown in Fig. 4 for the electrodes of 50 and 290 cm^2. The MEA SH1 was prepared with commercial components, electrodes of carbon paper among them. During the characterisation phase, the MEA SH1 showed a performance comparable to the commercial
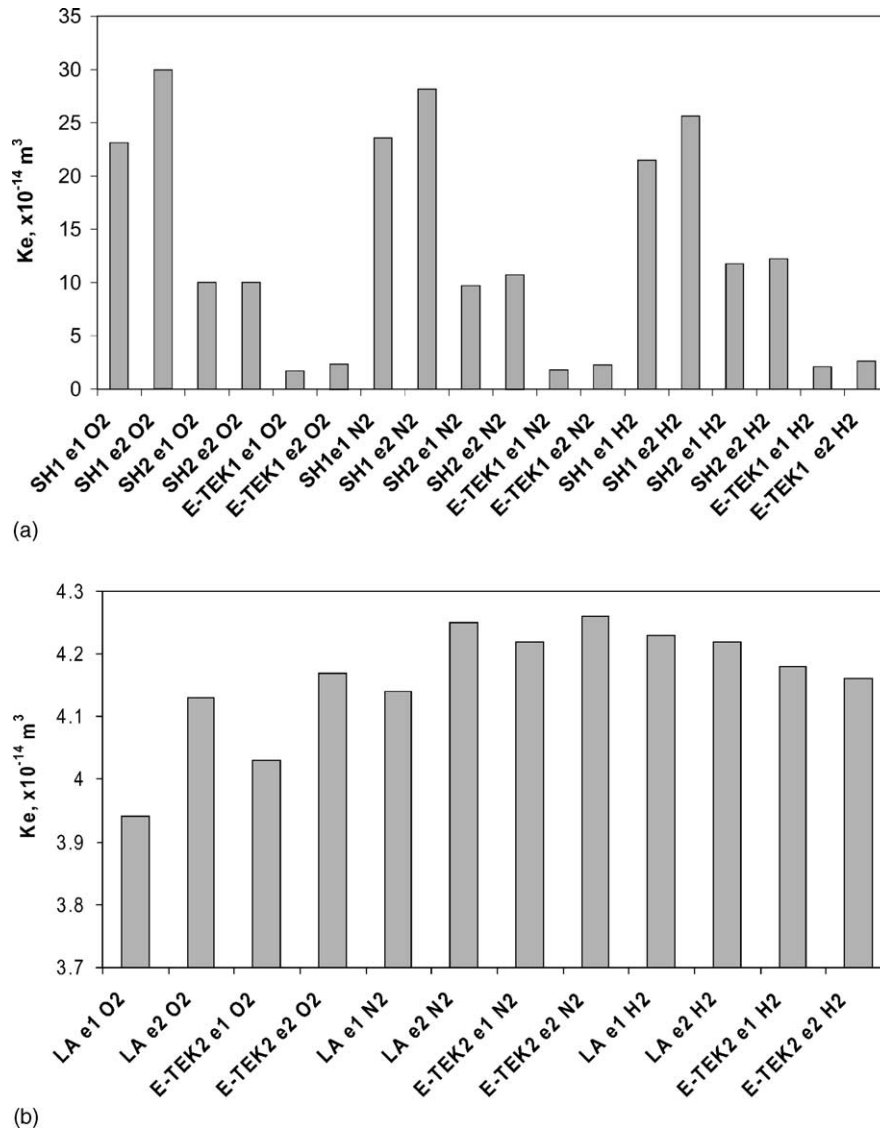
Fig. 4. The $K \cdot e$ values of the MEAs of: (a) 50 cm^2 and (b) 290 cm^2 with electrodes of carbon paper (SH1, LA) and carbon cloth (E-TEK1, E-TEK2, LA).

MEA from ElectroChem (EC). Hence, it is assumed that the $K \cdot e$ values measured with the MEA SH1 represent reasonably well the permeability of the electrodes of the MEA EC.

For a given MEA, small differences in the $K \cdot e$ values of the two electrodes (e1 and e2) can be observed in Fig. 4. The largest difference, nearly 20%, corresponds to the MEA SH1, the one with the most permeable electrodes. Moreover, for a given electrode, similar values of the product $K \cdot e$ were obtained with N$_2$, O$_2$ and H$_2$; the differences were inferior to 10% in all the cases. The electrodes of carbon paper showed higher permeabilities than the electrodes of carbon cloth in the MEAs of 50 cm^2. Nonetheless, similar permeabilities were found for the two types of electrodes in the MEAs of 290 cm^2. In particular, the $K \cdot e$ values correspondent to the E-TEK electrodes, i.e. carbon cloth 40 wt.% hydrophobic, compare quite well with those estimated by other authors [15].

4. Conclusions

The major conclusion were drawn from this work is stated here: the effects of the permeability of the electrodes and the type of gas flow distributor on the fuel cell performance are tightly linked to each other. In particular, the effect of the electrode permeability on the PEMFC performance depends strongly upon the flow-field pattern. This effect is not meaningful in the case of grooved plates, but it is rather significant in the case of solid plates. With the solid plates, the MEAs performed consistently with the gas permeability values of the electrodes measured experimentally. In general, the performance of the fuel cell with solid plates declines when the permeability of the electrodes decreases.

Furthermore, in the range of current densities covered here, up to 300 mA/cm^2, the MEAs with the more permeable electrodes performed comparably with either grooved plates

or solid plates. The less permeable ones were the electrodes of carbon cloth with 40 wt.% of hydrophobic material present in the MEAs provided by E-TEK. In this case, noticeably high diffusion losses were observed with the solid plates as compared to the grooved plates, particularly when air was used as oxidant. Therefore, the use of highly permeable electrodes, mainly carbon paper, is recommended when solid plates are used as gas flow distributor. With grooved plates, either carbon paper or carbon cloth can be used indistinctly.

Acknowledgements

References

[1] M. Uchida, Y. Fukuoka, Y. Sugawara, H. Ohara, A. Ohta, J. Electrochem. Soc. 145 (1998) 3708–3713.

[2] J.M. Song, S.Y. Cha, W.M. Lee, J. Power Sources 94 (2001) 78–84.

[3] E. Passalacqua, G. Squadrito, F. Lufrano, A. Patti, L. Giorgi, J. Appl. Electrochem. 31 (2001) 449–454.

[4] S.D. Thompson, L.R. Jordan, M. Forsyth, Electrochem. Acta 46 (2001) 1657–1663.

[5] S.-J. Shin, J.-K. Lee, H.-Y. Ha, S.-A. Hong, H.-S. Chun, I.-H. Oh, J. Power Sources 94 (2001) 78–84.

[6] V.A. Paganin, E.A. Ticianelly, E.R. Gonzalez, J. Appl. Electrochem. 26 (1996) 297–304.

[7] E. Passalacqua, I. Gatto, F. Lufrano, A. Patti, G. Squadrito, in: Proceedings of the 2000 Fuel Cell Seminar, Portland, OR, USA, 30 October–2 November 2000, pp. 118–121 (Abstracts).

[8] M.J. Escudero, E. Hontañón, S. Schwartz, M. Boutonnet, L. Daza, J. Power Sources 106 (2002) 206–214.

[9] C.S. Kong, D.-Y. Kim, H.-K. Lee, Y.-G. Shul, T.-H. Lee, J. Power Sources 108 (2002) 185–191.

[10] T.E. Springer, T.A. Zawodzinski, M.S. Wilson, S. Gottesfeld, J. Electrochem. Soc. 143 (1996) 587–599.

[11] B. Mueller, T. Zawodzinski, J. Bauman, F. Uribe, S. Gottesfeld, in: The Electrochemical Society Proceedings, vol. 98–27, 1998, Pennington, NJ, USA.

[12] J. Moreira, P.J. Sebastian, A.L. Ocampo, R.H. Castellanos, in: Proceedings of the 200th Meeting of the Abstracts Book of Electrochemical Society, San Francisco, CA, USA, September 2001.

[13] M.J. Escudero, E. Hontañón, P.L. García-Ybarra, L. Daza, in: Proceedings of the 2000 Fuel Cell Seminar, Portland, OR, USA, 30 October–2 November 2000, pp. 302–304 (Abstracts).

[14] E. Hontañón, M.J. Escudero, C. Bautista, P.L. García-Ybarra, L. Daza, J. Power Sources 86 (2000) 363–368.

[15] M. Mikkola, Master Thesis for Master of Science in Technology, Helsinki University of Technology, Finland, December 2001.